Cell Reports, Volume *42*

Supplemental information

Actin-dependent astrocytic infiltration is a key step for axon defasciculation during remodeling

Neta Marmor-Kollet, Victoria Berkun, Gideon Cummings, Hadas Keren-Shaul, Eyal David, Yoseph Addadi, and Oren Schuldiner

Supplemental information:

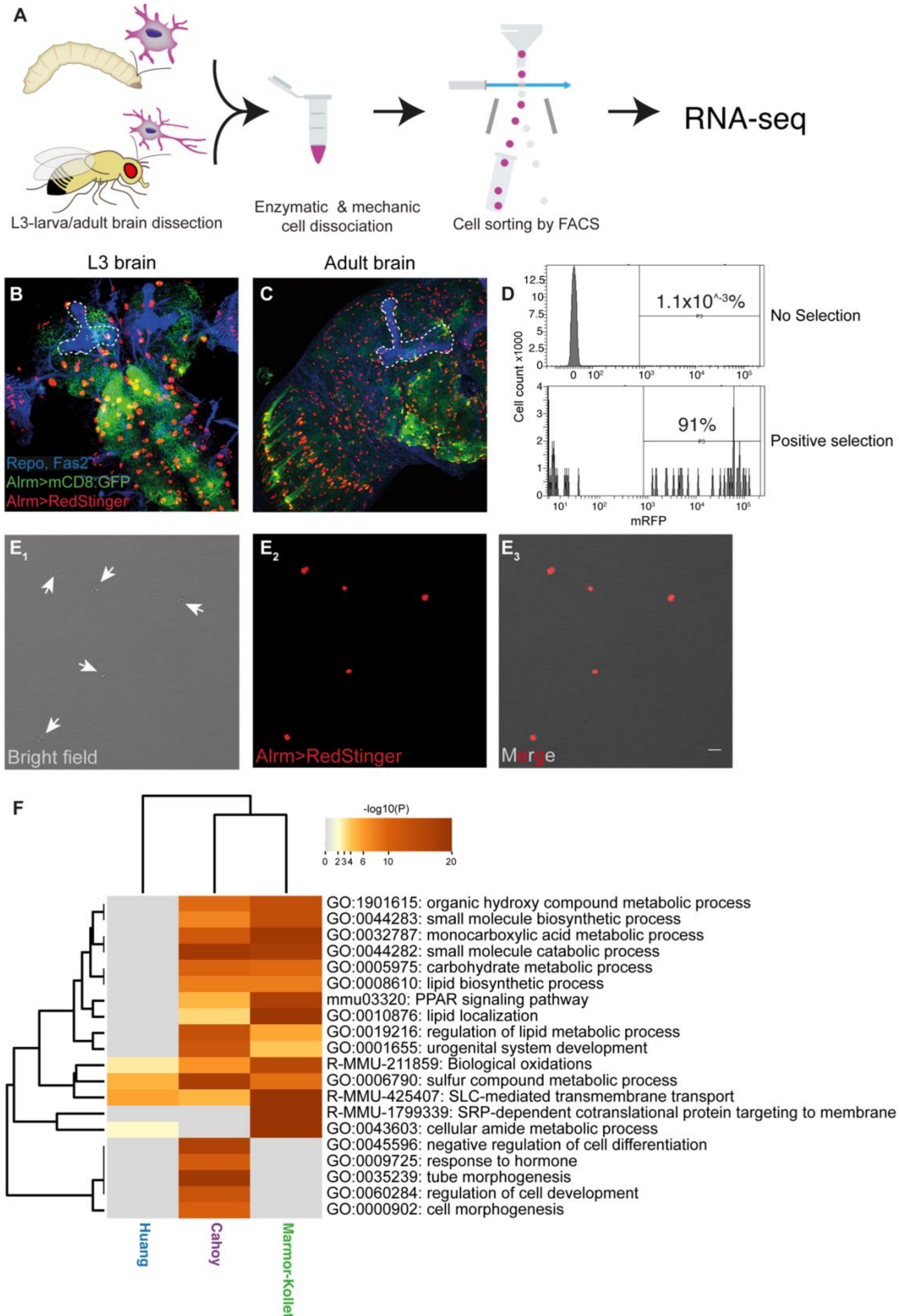

Figure S1: FACS-based purification of astrocyte-like glial cells, related to Figure 1.

(A) A scheme describing the cell labeling and purification protocol. (B-C) Confocal Z projections of 3rd instar larva (L3, B) and adult WT brains (C). Alrm-Gal4 drives the expression of membranal CD8::GFP as well as nuclear RedStinger specifically in astrocytes. Blue represents the combined antibody staining of Fas2 and Repo, which mark γ + α/β axons, and glia nuclei, respectively. KC axons are highlighted by a dashed white line. (D) FACS histogram plots of RFP positive astrocyte-like glial cells before and after positive selection. Sorting the cells by FACS yielded more than 90% enrichment. (E) Plated sorted cells confirm viability and RedStinger expression of sorted cells. White arrowheads indicate cells in bright field. Scale bar is 5μm. (F) Heatmap of selected enriched GO-terms in three astrocyte transcriptomic data sets – murine astrocytes (Cahoy et al., 2008), and adult *Drosophila* astrocytes (Huang et al., 2015, this manuscript), analyzed via (Zhou et al., 2019).

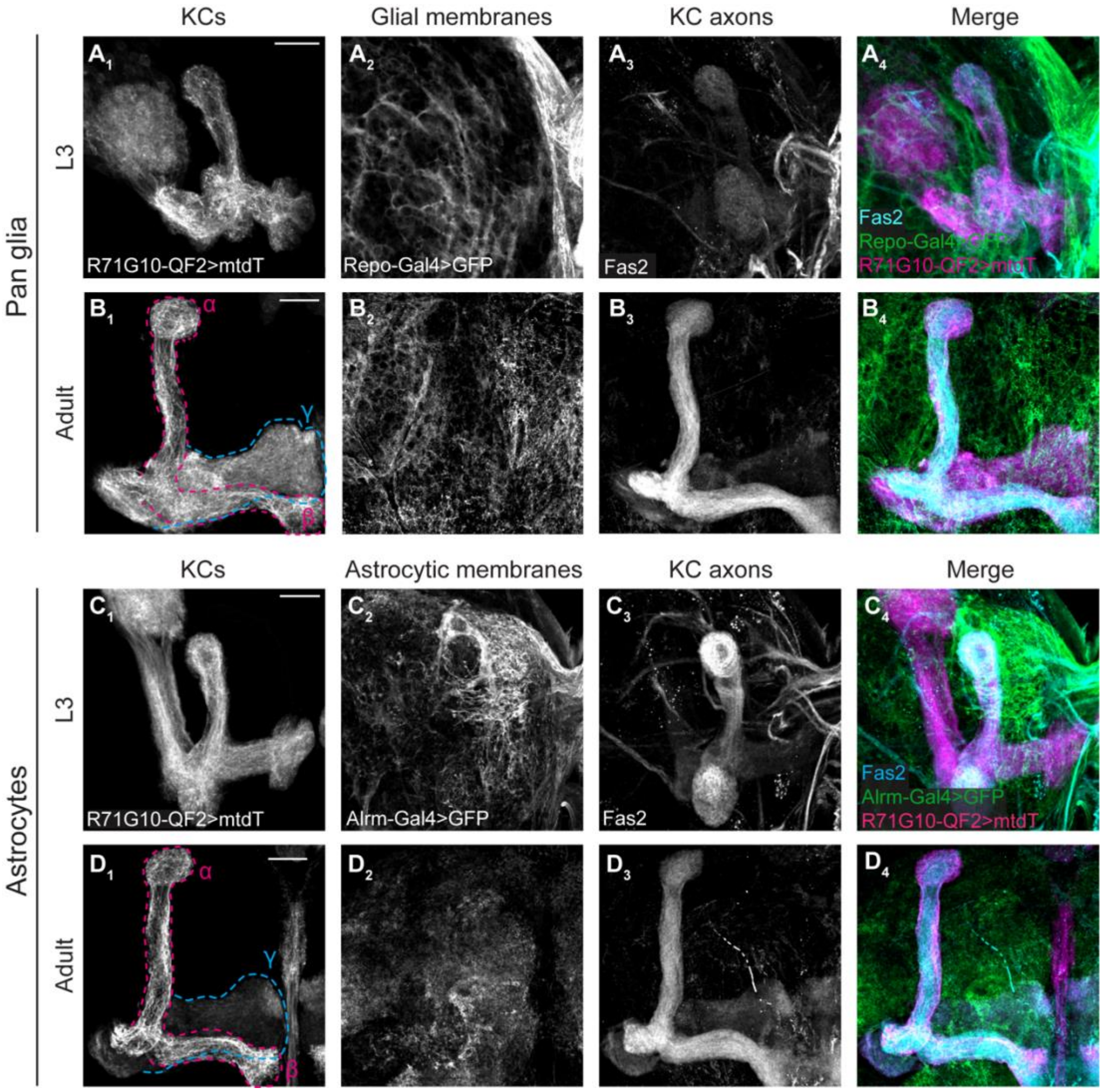

<u>Figure S2</u>: Two-binary expression systems enable the simultaneous manipulation of glia and KCs, related to Figure 2.

(A-D) Confocal Z-projections of 3rd instar larva (L3; A, C) and adult brains (B, D) expressing myristylated tandem Tomato (mtdT::3xHA; magenta or gray in A_1-D_1) driven by R71G10-QF2 in γ and in adult also in α/β-KCs as well as membrane-bound GFP (mCF8::GFP, green or gray in A_2-D_2) driven by Repo-Gal4 in all glia (A-B) or Alrm-Gal4, in astrocytes (C-D). Fas2 (cyan, gray in A_3-D_3); The γ-lobe is highlighted by a blue dashed line (B); The α/β lobes are highlighted by a magenta dashed line (D). Scale bar is 20μm.

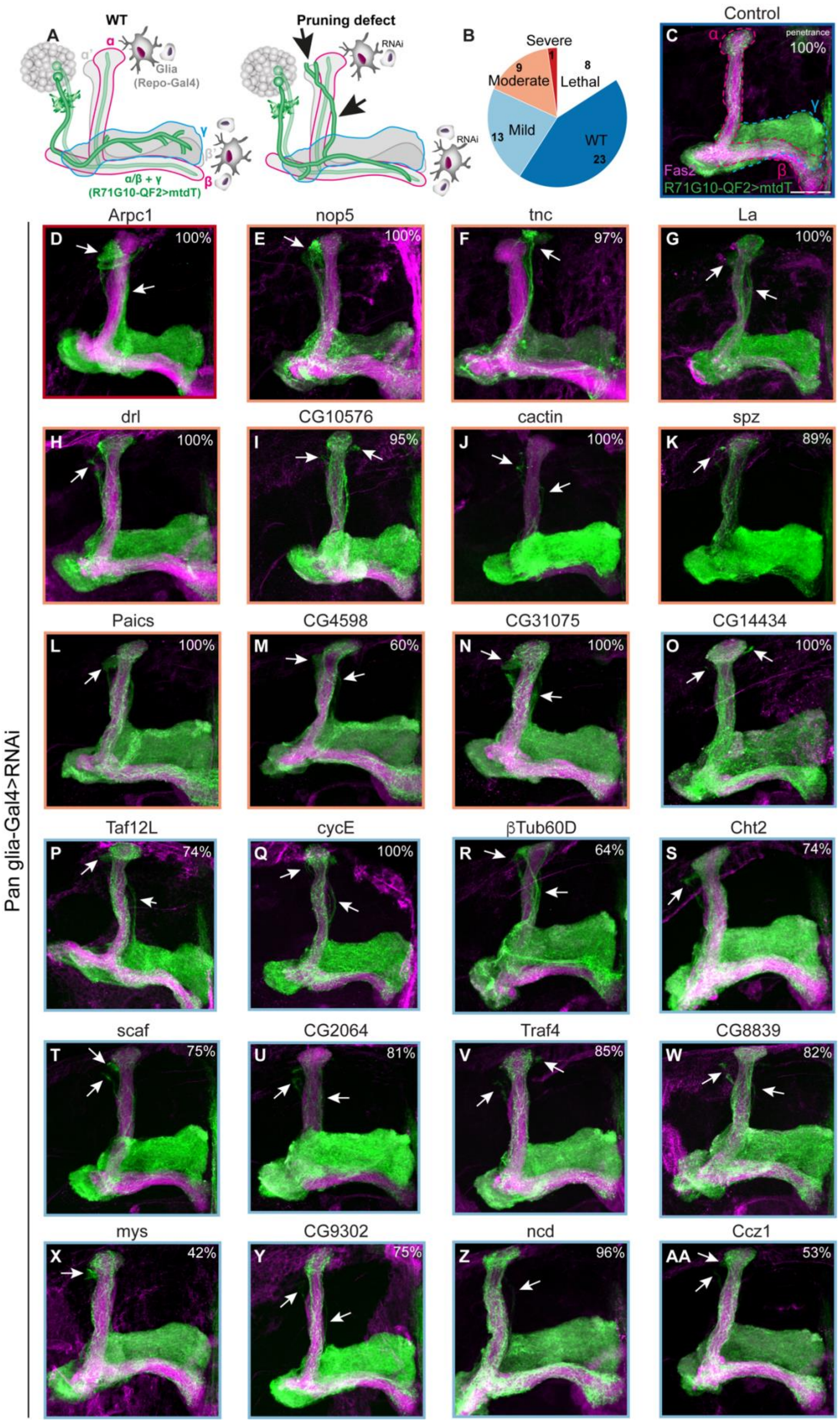

A
WT
α
α'
Glia
(Repo-Gal4)
γ
β'
α/β + γ
(R71G10-QF2>mtdT)
β
Pruning defect
RNAi
RNAi
B
Severe
1
9
Moderate
8
Lethal
13
Mild
WT
23
Control
C
α
penetrance
100%
γ
Fas2
β
R71G10-QF2>mtdT
Arpc1
D
100%
nop5
E
100%
tnc
F
97%
La
G
100%
drl
H
100%
CG10576
I
95%
cactin
J
100%
spz
K
89%
Paics
L
100%
CG4598
M
60%
CG31075
N
100%
CG14434
O
100%
Taf12L
P
74%
cycE
Q
100%
βTub60D
R
64%
Cht2
S
74%
scaf
T
75%
CG2064
U
81%
Traf4
V
85%
CG8839
W
82%
mys
X
42%
CG9302
Y
75%
ncd
Z
96%
Ccz1
AA
53%
Pan glia-Gal4>RNAi

<u>Figure S3</u>: Primary screen for glial genes required for γ axon pruning, related to Figure 2.

(A) A schematic representation of the experimental design and phenotypic outcomes of the primary RNAi screen. RNAi species targeting candidate genes were driven in glia by Repo-Gal4 (gray cells). γ-axon pruning phenotype was examined in adult brains via the expression of myristylated tandem Tomato (mtdT; green) driven by R71G10-QF2. Left: WT, all γ axons were pruned during pupal stages, and regrew to form the adult specific medial γ lobe (blue outline). Note that R71G10-QF2 is also often expressed in α/β neurons (light green) which are additionally strongly positive to Fas2 (magenta outline). Right: Pruning defect, some γ axons were not pruned, remanent of larval projections is visible outside the highly fasciculated α axon bundle (arrows). (B) a pie chart depicting the ratios between the different primary screen phenotypes. WT = wild type. Mild-moderate-severe – degrees of pruning defect. (C-AA) Confocal Z-projections of adult brains either expressing mtdT::3xHA driven by R71G10-QF2 and mCD8::GFP driven by Repo-Gal4 (C) or (D-AA) additionally expressing RNAi for Actin-related protein 2/3 complex, subunit 1 (Arpc1; D); nop5 (E); tenectin (tnc; F); LA autoantigen-like (LA; G); derailed (drl; H); CG10576 (I); cactin (J); spätzle (spz; K); PAICS bifunctional enzyme (Paics; L); CG4598 (M); CG31075 (N); CG14434 (O); TBP-associated factor 30kD subunit α-2 (Taf12L; P); Cyclin E (CycE; Q); β -Tubulin at 60D (β-tub60D; R); Chitinase 2 (Cht2; S); scarface (scaf; T); CG2064 (U); TNF-receptor-associated factor 4 (Traf4; V); CG8839 (W); myospheroid (mys; X); CG9302 (Y); non-claret disjunctional (ncd; Z); Caffeine, calcium, zinc sensitivity 1 (Ccz1; AA); In C, the γ-lobe is highlighted by a blue dashed line, the α/β lobes are highlighted by a magenta dashed line. Arrows demarcate unpruned axons. Frame color in C-AA represents their phenotype as depicted in B. Phenotypic penetrance is presented in percentage. Scale bar is 20 µm.

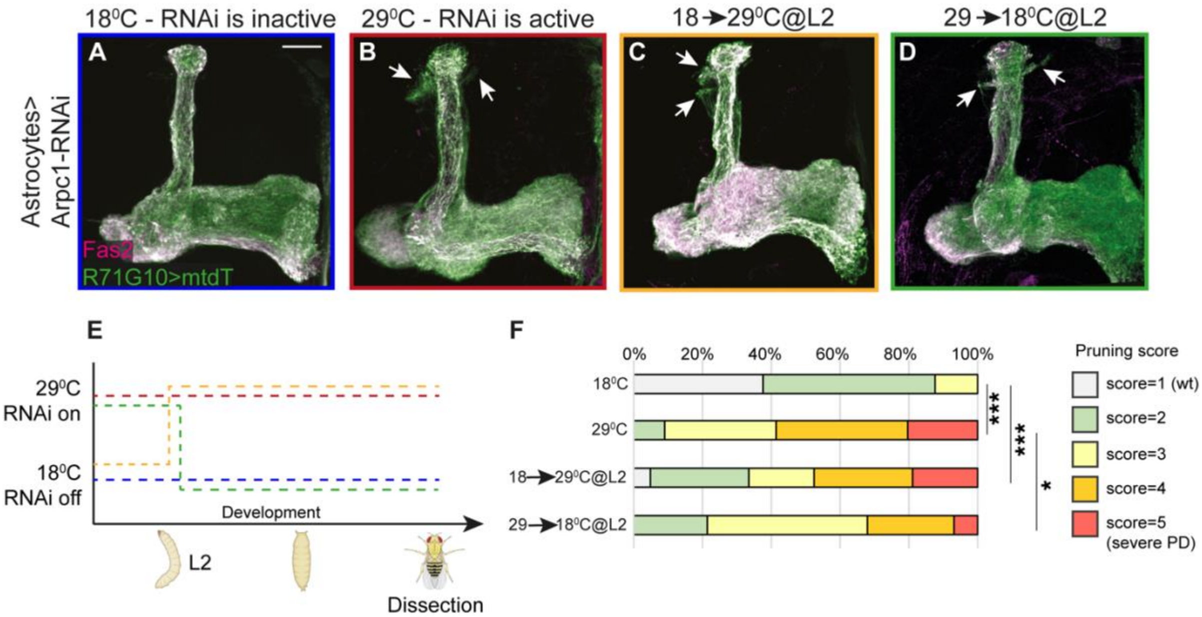

<u>Figure S4</u>: Astrocytic Arpc1 is required for γ axon pruning at the onset of metamorphosis. Related to Figure 3.

(A-D) Confocal Z-projections of adult brains expressing Gal80ts under the constitutive tubulin promoter, mCD8::GFP and Arpc1-RNAi driven by Alrm-Gal4, as well as mtdT::3xHA (green) driven by R71G10-QF2. Flies were raised at 18°C (inactive RNAi) or 29°C (active RNAi) as indicated and schematized in (E). (F) Quantification of the pruning defect phenotypes manifested in (A-D). Defects score from 1-5, 1 being WT and 5 being severe pruning defects. p values: 29^0C compared to 18^0C: p<0.001. 18^0C→29^0C compared to 18^0C: p<0.001. 29^0C→18^0C compared to 29^0C: p=0.036. Frame color in A-D represents the experimental design as depicted in E. White arrows indicate unpruned γ axons. mtdT::3xHA (green). Fas2 (magenta). Scale bar is 20μm.

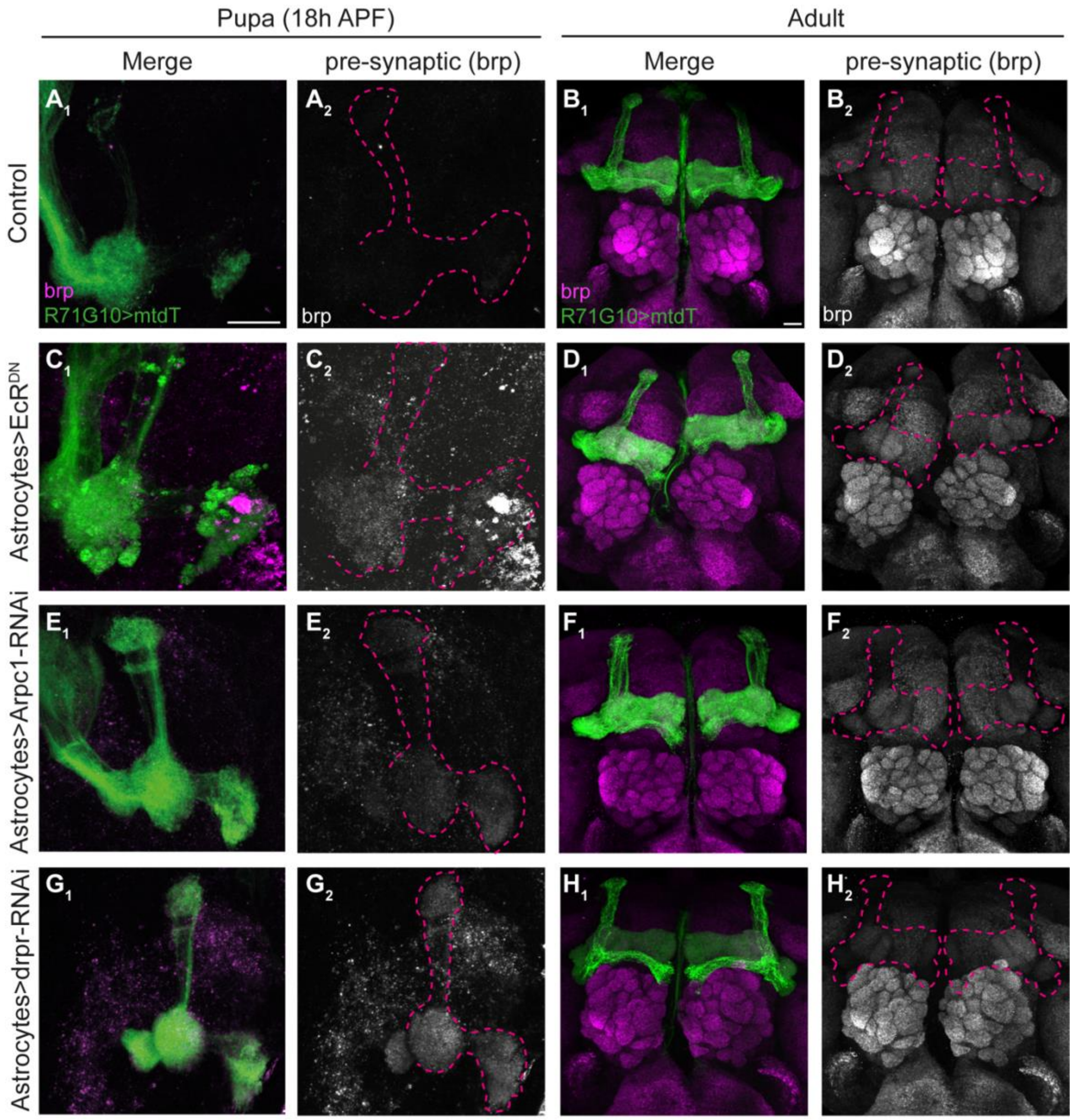

<u>Figure S5</u>: Astrocytic Arpc1 is required for synaptic clearance following axon pruning, related to Figure 3.

(A-H) Confocal Z-projections of 18h APF brains (A, C, E, G) or adult brains (B, D, F, H) expressing mtdT::3xHA driven by R71G10-QF2 and mCD8::GFP driven by Alrm-Gal4 (A, B) or additionally expressing EcR^{DN} (C-D), Arpc1-RNAi (E-F), or drpr-RNAi (G-H). Magenta dashed lines indicate KC axons. mtdT::3xHA (green). brp (anti-nc82, magenta or gray). Scale bar is 20μm.

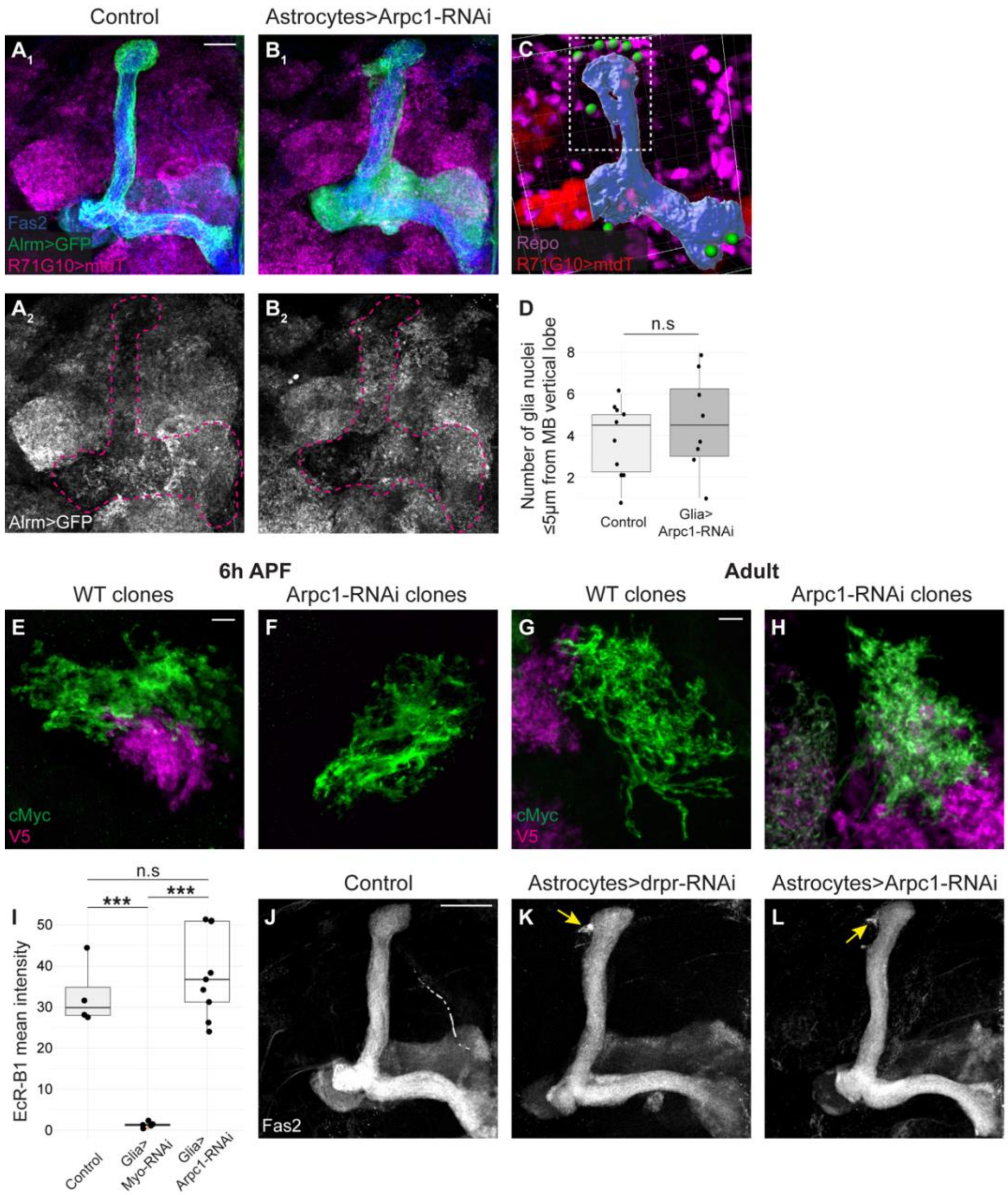

Figure S6: **Astrocytic membrane volume occupancy or migration are not affected by Arpc1-KD, related to Figure 4.**

(A-B) Confocal Z-projections of adult brains expressing mtdT::3xHA (green) driven by R71G10-QF2 and mCD8::GFP (magenta, gray) driven by Alrm-Gal4 (A), or additionally expressing Arpc1-RNAi (B). Dashed magenta outline represents KC axons according to mtdT::3xHA labeling. Fas2 (blue). Scale bar is 20µm. (C) Scheme of image analysis performed in (D) to quantify the number of glial nuclei within 5µm of the vertical axon lobe at 6h APF. (D) Analyses performed in Imaris, which demarcates KC axons surface (in blue) and proximal glial nuclei (green). Number of glia nuclei within 5µm of the vertical γ-KC axon bundle was not affected by Arpc1-KD. (E-H) Confocal

Z-projections of 6h APF (E-F) or adult (G-H) brains containing WT (E, G) or Arpc1-RNAi astrocytic MCFO clones (F, H) expressing cMyc and/or V5. (I) Quantification of EcR-B1 antibody mean fluorescent intensity in γ cell bodies at 0h APF in either Repo-Gal4 controls, or Repo-Gal4 driving myo-RNAi or Arpc1-RNAi, respectively. p-values compared to control: myo-RNAi – $p<0.001$. Arpc1-RNAi – p-value<0.001. n.s - not significant. (J-L) Confocal Z-projections of adult brains expressing mtdT::3xHA driven by R71G10-QF2 and mCD8::GFP driven by Alrm-Gal4 (I), or additionally expressing drpr-RNAi (J), or Arpc1-RNAi (K). Fas2 (gray). Yellow arrows indicate unengulfed axonal debris. Scale bar is 20μm.

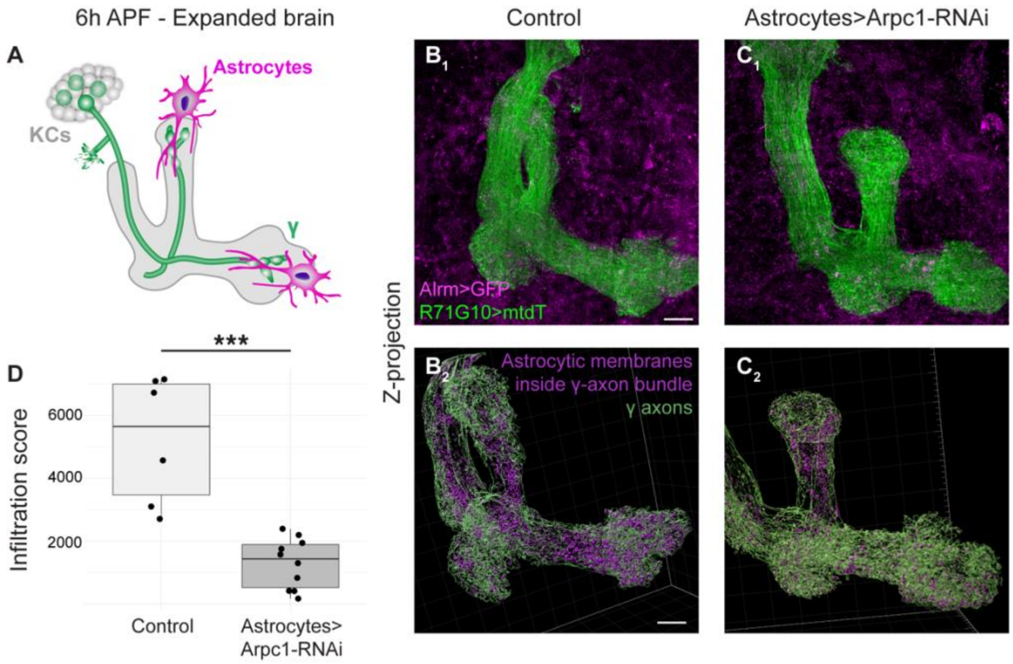

<u>Figure S7</u>: Expansion microscopy further validates Arpc1 requirement for astrocytic infiltration into the axon bundle at the onset of pruning, related to figure 5.

(A) A scheme of the MB at 6h APF highlighting the γ-KCs (magenta) and astrocytes (green). (B-C) Spinning disk confocal Z-projection images of 6h APF expanded brains expressing mtdT::3xHA (green) driven by R71G10-QF2 and mCD8::GFP (magenta) driven by Alrm-Gal4 (B_1), or additionally expressing Arpc1-RNAi (C_1). Scale bar is 20μm. Astrocytic infiltration into the axon bundle was analyzed in (B_2-C_2) using Imaris, where KC axons surface was demarcated in green and astrocytic membranes inside the axon surface were demarcated in magenta. (D) Quantification of lobe infiltration by astrocytes. p value<0.001.

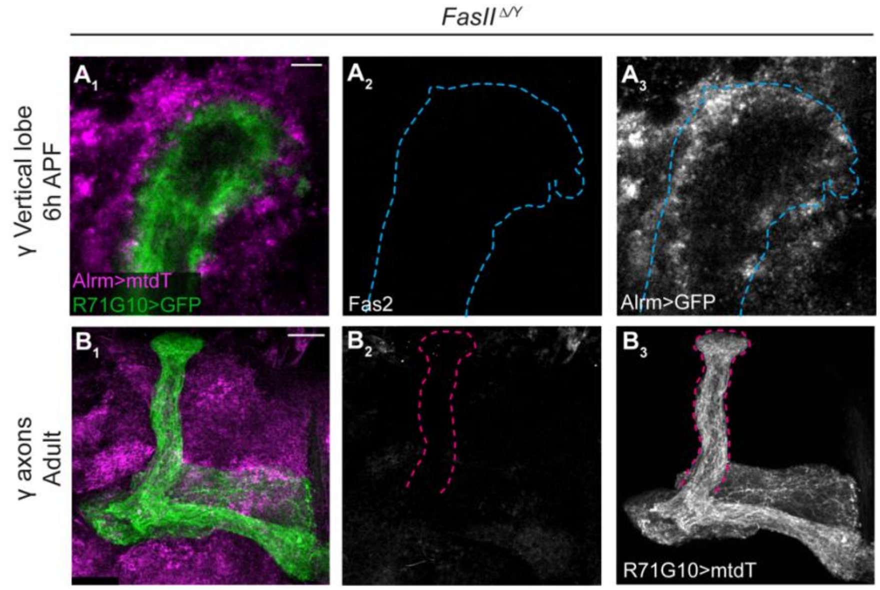

<u>Figure S8</u>: Loss of Fas2 does not induce pruning or infiltration defects on its own, related to Figure 6.

(A) Single confocal slices of 6h APF Fas2$^{\Delta TM\text{-}PA/Y}$ brain expressing mCD8::GFP (magenta or gray in A3) driven by Alrm-Gal4 while axons are labeled by mtdT::3xHA driven by R71G10-QF2 (green). (B) Confocal Z-projections of adult Fas2$^{\Delta TM\text{-}PA/Y}$ brain expressing mCD8::GFP driven by Alrm-Gal4 (magenta) while axons are labeled by mtdT::3xHA driven by R71G10-QF2 (green or gray in B3). Fas2 (gray in A2-B2); γ vertical lobe is highlighted by a blue dashed outline (A). The α lobe is highlighted by a magenta dashed line (B). Scale bar is 5μm (A) or 20μm (B).

FIGURE	GENOTYPE	n
Figure 2		
2C	+/+ or Y; R71G10-QF2, QUAS-mtdT/+; Alrm-Gal4, UAS-GFP, UAS-Dcr2/+	18
2D	+/y^1, v^1 or Y; R71G10-QF2, QUAS-mtdT/+; Alrm-Gal4, UAS-GFP, UAS-Dcr2/UAS-Arpc1-RNAi	21/21
2E	+/y^1, sc^*, v^1, sev^{21} or Y; R71G10-QF2, QUAS-mtdT/+; Alrm-Gal4, UAS-GFP, UAS-Dcr2/UAS-Ama-RNAi	12/12
2F	+/y^1, sc^*, v^1, sev^{21} or Y; R71G10-QF2, QUAS-mtdT/+; Alrm-Gal4, UAS-GFP, UAS-Dcr2/UAS-form3-RNAi	16/16
2G	+/y^1, sc^*, v^1, sev^{21} or Y; R71G10-QF2, QUAS-mtdT/+; Alrm-Gal4, UAS-GFP, UAS-Dcr2/UAS-PCNA-RNAi	18/18
2H	+/y^1, sc^*, v^1, sev^{21} or Y; R71G10-QF2, QUAS-mtdT/UAS-Dl-RNAi; Alrm-Gal4, UAS-GFP, UAS-Dcr2/+	15/15
2I	y, w/+; R71G10-QF2, QUAS-mtdT/+; Alrm-Gal4, UAS-GFP, UAS-Dcr2/UAS-fabp-RNAi	5/14
2J	+/y^1, sc^*, v^1, sev^{21} or Y; R71G10-QF2, QUAS-mtdT/+; Alrm-Gal4, UAS-GFP, UAS-Dcr2/ UAS-nop5-RNAi	5/8
2K	+/y^1, sc^*, v^1, sev^{21} or Y; R71G10-QF2, QUAS-mtdT/+; Alrm-Gal4, UAS-GFP, UAS-Dcr2/ UAS-Ssrp-RNAi	27/28
2L	+/y^1, sc^*, v^1, sev^{21} or Y; R71G10-QF2, QUAS-mtdT/+; Alrm-Gal4, UAS-GFP, UAS-Dcr2/ UAS-spz-RNAi	12/14
2M	+/y^1, sc^*, v^1, sev^{21} or Y; R71G10-QF2, QUAS-mtdT/+; Alrm-Gal4, UAS-GFP, UAS-Dcr2/ UAS-Fib-RNAi	14/16
2N	+/y^1, sc^*, v^1, sev^{21} or Y; R71G10-QF2, QUAS-mtdT/+; Alrm-Gal4, UAS-GFP, UAS-Dcr2/ UAS- CG10576-RNAi	6/12
2O	+/y^1, v^1 or Y; R71G10-QF2, QUAS-mtdT/+; Alrm-Gal4, UAS-GFP, UAS-Dcr2/UAS-Traf4-RNAi	10/14
Figure 3		
3B	+/+ or Y; R71G10-QF2, QUAS-mtdT/+; Alrm-Gal4, UAS-GFP, UAS-Dcr2/+	18

3C	+/y^1, v^1 or Y ; R71G10-QF2, QUAS-mtdT/+; Alrm-Gal4, UAS-GFP, UAS-Dcr2/UAS-Arpc1-RNAi	21/21
3D	+/y^1, v^1 or Y; R71G10-QF2, QUAS-mtdT/+; Alrm-Gal4, UAS-GFP, UAS-Dcr2/UAS-Arp2-RNAi	34/34
3E	+/y^1, v^1 or Y; R71G10-QF2, QUAS-mtdT/UAS-Arp3-RNAi; Alrm-Gal4, UAS-GFP, UAS-Dcr2/+	25/30
3F	+/y^1, v^1 or Y; R71G10-QF2, QUAS-mtdT/UAS-Arpc2-RNAi; Alrm-Gal4, UAS-GFP, UAS-Dcr2/ +	30/30
3G	+/y^1, v^1 or Y; R71G10-QF2, QUAS-mtdT/+; Alrm-Gal4, UAS-GFP, UAS-Dcr2/UAS-Arpc3A - RNAi	28/28
3H	+/y^1, v^1 or Y; R71G10-QF2, QUAS-mtdT/+; Alrm-Gal4, UAS-GFP, UAS-Dcr2/UAS-Arpc3B - RNAi	27/28
3I	+/y^1, v^1 or Y; R71G10-QF2, QUAS-mtdT/UAS-WASp-RNAi; Alrm-Gal4, UAS-GFP, UAS-Dcr2/+	26/28
3J	+/y^1, sc^*, v^1, sev^{21} or Y; R71G10-QF2, QUAS-mtdT/UAS-wash RNAi; Alrm-Gal4, UAS-GFP, UAS-Dcr2/+	25/27
3K	+/y^1, sc^*, v^1, sev^{21} or Y; R71G10-QF2, QUAS-mtdT/UAS-SCAR RNAi; Alrm-Gal4, UAS-GFP, UAS-Dcr2/+	10/12
3L	+/y^1, sc^*, v^1, sev^{21} or Y; R71G10-QF2, QUAS-mtdT/+; Alrm-Gal4, UAS-GFP, UAS-Dcr2/UAS-form3 RNAi	16/16
3M	+/y^1, sc^*, v^1, sev^{21} or Y; R71G10-QF2, QUAS-mtdT/+; Alrm-Gal4, UAS-GFP, UAS-Dcr2/UAS-capu RNAi	26/26
3N	+/y^1, sc^*, v^1, sev^{21} or Y; R71G10-QF2, QUAS-mtdT/+; Alrm-Gal4, UAS-GFP, UAS-Dcr2/UAS-DAAM-RNAi	30/30
3O	+/y^1, v^1 or Y; R71G10-QF2, QUAS-mtdT/+; Alrm-Gal4, UAS-GFP, UAS-Dcr2/UAS-dia-RNAi	28/28
3P	+/y^1, sc^*, v^1, sev^{21} or Y; R71G10-QF2, QUAS-mtdT/+; Alrm-Gal4, UAS-GFP, UAS-Dcr2/UAS-Frl RNAi	34/34
3Q	+/y^1, v^1 or Y; R71G10-QF2, QUAS-mtdT/UAS-Fhos-RNAi; Alrm-Gal4, UAS-GFP, UAS-Dcr2/+	32/32

Figure 4		
4C	y^1, w^*, hsflp, CD8/+ OR Y; Gal80, 40A/40A, G13; Alrm-Gal4/+	10

4D	y^1, w^*, hsflp, CD8/+ OR Y; Gal80, 40A, G13 /Arpc1^{Q25st}, 40A; Alrm-Gal4/+	10
4E	+/+ or Y; R71G10-QF2, QUAS-mtdT/+; Repo-Gal4, UAS-GFP/+	4
4F	+/y^1, v^1 or Y ; R71G10-QF2, QUAS-mtdT/+; Repo-Gal4, UAS-GFP/ UAS-Myo-RNAi	5
4G	+/y^1, v^1 or Y ; R71G10-QF2, QUAS-mtdT/+; Repo-Gal4, UAS-GFP/UAS-Arpc1-RNAi	9
4I	+/+ or Y; R71G10-QF2, QUAS-mtdT/+; Alrm-Gal4, UAS-GFP, UAS-Dcr2/+	18
4J	+/y^1, v^1 or Y; R71G10-QF2, QUAS-mtdT/+; Alrm-Gal4, UAS-GFP, UAS-Dcr2/UAS-Arpc1-RNAi	26
Figure 5		
5B	+/+ or Y; R71G10-QF2, QUAS-mtdT/+; Alrm-Gal4, UAS-GFP, UAS-Dcr2/+	20
5C	+/+ or Y; R71G10-QF2, QUAS-mtdT/+; Alrm-Gal4, UAS-GFP, UAS-Dcr2/UAS-Arpc1-RNAi	26

Figure 6		
6A	FM7 or fas2$^{\Delta TM-PA}$/+; R71G10-QF2, QUAS-mtdT/+; Alrm-Gal4, UAS-GFP, UAS-Dcr2/UAS-Arpc1-RNAi	10
6B, E	fas2$^{\Delta TM-PA}$/Y; R71G10-QF2, QUAS-mtdT/+; Alrm-Gal4, UAS-GFP, UAS-Dcr2/UAS-Arpc1-RNAi	10, 20 respectively
6D	FM7/+; R71G10-QF2, QUAS-mtdT/+; Alrm-Gal4, UAS-GFP, UAS-Dcr2/UAS-Arpc1-RNAi	20
Figure 7		
6A, D	UAS-bsk^{DN}/+ or Y; 201Y-Gal4, UAS-CD8:GFP/+; Alrm-QF2, QUAS-mtdT::3xHA/+	14, 12, respectively
6B, E	UAS-bsk^{DN}/+ or Y; 201Y-Gal4, UAS-CD8:GFP/UAS-NCAM^{140}; Alrm-QF2, QUAS-mtdT::3xHA/+	8, 12, respectively

Figure S1		
S1A, B, D, E	UAS-GFP; Alrm-Gal4; UAS-RedStinger/TM6, tb, hu	
Figure S2		

S2A, B	y, w/+; R71G10-QF2, QUAS-mtdT/+; Repo-Gal4, UAS-GFP/+.	
S2C, D	y, w/+; R71G10-QF2, QUAS-mtdT/+; Alrm-Gal4, UAS-GFP, UAS-Dcr2/+.	

Figure S3		
S3C	+/+ or Y; R71G10-QF2, QUAS-mtdT/+; Repo-Gal4, UAS-GFP/+	12
S3D	+/y^{1}, v^{1} or Y ; R71G10-QF2, QUAS-mtdT/+; Repo-Gal4, UAS-GFP/UAS-Arpc1-RNAi	24/24
S3E	+/y^{1}, sc^{*}, v^{1}, sev^{21} or Y; R71G10-QF2, QUAS-mtdT/ UAS-nop5-RNAi; Repo-Gal4, UAS-GFP/+	8/8
S3F	+/y^{1}, v^{1} or Y ; R71G10-QF2, QUAS-mtdT/UAS-tnc-RNAi; Repo-Gal4, UAS-GFP/+	14/16
S3G	+/y^{1}, sc^{*}, v^{1}, sev^{21} or Y; R71G10-QF2, QUAS-mtdT/UAS-La-RNAi; Repo-Gal4, UAS-GFP/+	24/24
S3H	+/y^{1}, sc^{*}, v^{1}, sev^{21} or Y; R71G10-QF2, QUAS-mtdT/+; Repo-Gal4, UAS-GFP/UAS-drl-RNAi	8/8
S3I	+/y^{1}, sc^{*}, v^{1}, sev^{21} or Y; R71G10-QF2, QUAS-mtdT/+; Repo-Gal4, UAS-GFP/UAS-CG10576-RNAi	14/16
S3J	+/y^{1}, sc^{*}, v^{1}, sev^{21} or Y; R71G10-QF2, QUAS-mtdT/UAS-cactin-RNAi; Repo-Gal4, UAS-GFP/+	15/15
S3K	+/y^{1}, sc^{*}, v^{1}, sev^{21} or Y; R71G10-QF2, QUAS-mtdT/+; Repo-Gal4, UAS-GFP/UAS-spz-RNAi	14/14
S3L	+/y^{1}, sc^{*}, v^{1}, sev^{21} or Y; R71G10-QF2, QUAS-mtdT/ UAS- Paics-RNAi; Repo-Gal4, UAS- GFP/+	14/14
S3M	+/y^{1}, v^{1}/+ or Y; R71G10-QF2, QUAS-mtdT/UAS-CG4598-RNAi; Repo-Gal4, UAS- GFP/+	12/20
S3N	+/y^{1}, sc^{*}, v^{1}, sev^{21} or Y; R71G10-QF2, QUAS-mtdT/+; Repo-Gal4, UAS-GFP/ UAS-CG31075-RNAi	26/26
S3O	+/y^{1}, sc^{*}, v^{1}, sev^{21} or Y; R71G10-QF2, QUAS-mtdT/ UAS-CG14434-RNAi; Repo-Gal4, UAS-GFP/+	24/24
S3P	+/y^{1}, sc^{*}, v^{1}, sev^{21} or Y; R71G10-QF2, QUAS-mtdT/UAS-Taf12L-RNAi; Repo-Gal4, UAS-GFP/+	20/27
S3Q	+/y^{1}, sc^{*}, v^{1}, sev^{21} or Y; R71G10-QF2, QUAS-mtdT/+; Repo-Gal4, UAS-GFP/UAS-cycE-RNAi	27/27

S3R	+/y^1, sc^*, v^1, sev^{21} or Y; R71G10-QF2, QUAS-mtdT/UAS-βtub60D-RNAi; Repo-Gal4, UAS-GFP/+	9/14
S3S	+/y^1, v^1or Y; R71G10-QF2, QUAS-mtdT/UAS-Cht2-RNAi; Repo-Gal4, UAS-GFP/+	20/27
S3T	+/y^1, sc^*, v^1, sev^{21} or Y; R71G10-QF2, QUAS-mtdT/UAS-scaf-RNAi; Repo-Gal4, UAS-GFP/+	9/12
S3U	+/y^1, sc^*, v^1, sev^{21} or Y; R71G10-QF2, QUAS-mtdT/+; Repo-Gal4, UAS-GFP/UAS-CG2064-RNAi	13/16
S3V	+/y^1, v^1 or Y ; R71G10-QF2, QUAS-mtdT/+; Repo-Gal4, UAS-GFP/AUS-Traf4-RNAi	17/20
S3W	+/y^1, sc^*, v^1, sev^{21} or Y; R71G10-QF2, QUAS-mtdT/+; Repo-Gal4, UAS-GFP/UAS-CG8839-RNAi	9/11
S3X	+/y^1, sc^*, v^1, sev^{21} or Y; R71G10-QF2, QUAS-mtdT/+; Repo-Gal4, UAS-GFP/UAS-mys-RNAi	5/12
S3Y	+/y^1, sc^*, v^1, sev^{21} or Y; R71G10-QF2, QUAS-mtdT/UAS-CG9302-RNAi; Repo-Gal4, UAS-GFP/+	15/20
S3Z	+/y^1, v^1 or Y; R71G10-QF2, QUAS-mtdT/UAS-ncd-RNAi; Repo-Gal4, UAS-GFP/+	22/23
S3AA	+/y^1, v^1 or Y; R71G10-QF2, QUAS-mtdT/UAS-Ccz1-RNAi; Repo-Gal4, UAS-GFP/+	17/31
<u>Figure S4</u>		
S4A-D	y, v/+ or Y; R71G10-QF2, QUAS-mtdT/$Gal80^{ts}$; Alrm-Gal4, UAS-GFP, UAS-Dcr2/UAS-Arpc1-RNAi	24, 34, 21, 28 respectively
<u>Figure S5</u>		
S5A, B	+/+ or Y; R71G10-QF2, QUAS-mtdT/+; Alrm-Gal4, UAS-GFP, UAS-Dcr2/+	8
S5C, D	+/+ or Y; R71G10-QF2, QUAS-mtdT/sp or CyO; Alrm-Gal4, UAS-GFP, UAS-Dcr2/UAS-EcR^{DN}	18/18
S5E, F	+/+ or Y; R71G10-QF2, QUAS-mtdT/+; Alrm-Gal4, UAS-GFP, UAS-Dcr2/UAS-Arpc1-RNAi	5/11
S5G, H	+/+ or Y; R71G10-QF2, QUAS-mtdT/+; Alrm-Gal4, UAS-GFP, UAS-Dcr2/UAS-drpr-RNAi	10/12

Figure S6		
S6A	+/+ or Y; R71G10-QF2, QUAS-mtdT/+; Alrm-Gal4, UAS-GFP, UAS-Dcr2/+	18
S6B	+/y^1, v^1 or Y; R71G10-QF2, QUAS-mtdT/+; Alrm-Gal4, UAS-GFP, UAS-Dcr2/UAS-Arpc1-RNAi	21/21
S6C	+/y^1, v^1 or Y; R71G10-QF2, QUAS-mtdT/+; Repo-Gal4, UAS-GFP/UAS-Arpc1-RNAi	
S6E, G	hsflpG5/+ or Y; 10xUAS(FRT-stop)myr::smGdP-V5-THS-10xUAS(FRT-stop)myr::smGdP-cMyc/+; Alrm-Gal4/TM3, sb	3, 8, respectively
S6F, H	hsflpG5/+ or Y; 10xUAS(FRT-stop)myr::smGdP-V5-THS-10xUAS(FRT-stop)myr::smGdP-cMyc/+; Alrm-Gal4/UAS-Arpc1-RNAi	2, 8, respectively
S6J	+/+ or Y; R71G10-QF2, QUAS-mtdT/+; Alrm-Gal4, UAS-GFP, UAS-Dcr2/+	18
S6K	+/y^1, sc^*, v^1, sev^{21} or Y; R71G10-QF2, QUAS-mtdT/+; Alrm-Gal4, UAS-GFP, UAS-Dcr2/UAS-drpr-RNAi	21/21
S6L	+/y^1, v^1 or Y; R71G10-QF2, QUAS-mtdT/+; Alrm-Gal4, UAS-GFP, UAS-Dcr2/UAS-Arpc1-RNAi	20/20

Figure S7		
S7B	+/+ or Y; R71G10-QF2, QUAS-mtdT/+; Alrm-Gal4, UAS-GFP, UAS-Dcr2/+	6
S7C	+/y^1, v^1 or Y; R71G10-QF2, QUAS-mtdT/+; Alrm-Gal4, UAS-GFP, UAS-Dcr2/UAS-Arpc1-RNAi	10

Figure S8		
S8A	$fas2^{\Delta TM\text{-}PA}$/Y; R71G10-QF2, QUAS-mtdT/+; Alrm-Gal4, UAS-GFP, UAS-Dcr2/sb	6
S8B	$fas2^{\Delta TM\text{-}PA}$/Y; R71G10-QF2, QUAS-mtdT/+; Alrm-Gal4, UAS-GFP, UAS-Dcr2/sb	10

Table S4: A list of full genotypes and sample sizes described throughout the paper.